Gαq-mediated calcium dynamics and membrane tension modulate neurite plasticity

Katherine M. Pearce[a,†], Miriam Bell[b,†], Will H. Linthicum[c], Qi Wen[c], Jagan Srinivasan[d], Padmini Rangamani[b,*], and Suzanne Scarlata[a,*]

[a]Department of Chemistry and Biochemistry, [c]Department of Biomedical Engineering, and [d]Department of Biology and Biotechnology, Worcester Polytechnic Institute, Worcester, MA 01609; [b]Mechanical and Aerospace Engineering Department, University of California, San Diego, La Jolla, CA 92093

ABSTRACT **The formation and disruption of synaptic connections during development are a fundamental step in neural circuit formation. Subneuronal structures such as neurites are known to be sensitive to the level of spontaneous neuronal activity, but the specifics of how neurotransmitter-induced calcium activity regulates neurite homeostasis are not yet fully understood. In response to stimulation by neurotransmitters such as acetylcholine, calcium responses in cells are mediated by the Gαq/phospholipase Cβ (PLCβ)/phosphatidylinositol 4,5-bisphosphate (PI(4,5)P_2) signaling pathway. Here, we show that prolonged Gαq stimulation results in the retraction of neurites in PC12 cells and the rupture of neuronal synapses by modulating membrane tension. To understand the underlying cause, we dissected the behavior of individual components of the Gαq/PLCβ/PI(4,5)P_2 pathway during retraction and correlated these with the retraction of the membrane and cytoskeletal elements impacted by calcium signaling. We developed a mathematical model that combines biochemical signaling with membrane tension and cytoskeletal mechanics to show how signaling events are coupled to retraction velocity, membrane tension, and actin dynamics. The coupling between calcium and neurite retraction is shown to be operative in the *Caenorhabditis elegans* nervous system. This study uncovers a novel mechanochemical connection between Gαq/PLCβ /PI(4,5)P_2 that couples calcium responses with neural plasticity.**

Monitoring Editor
John York
Vanderbilt University

Received: Sep 18, 2019
Revised: Dec 2, 2019
Accepted: Dec 5, 2019

INTRODUCTION

Throughout the course of an organism's life, different neuronal connections break and reform to generate new electrical patterns that allow optimal function during development and through adulthood. This plasticity of neuronal connections allows the rewiring of circuitry necessary for memory and learning (e.g., Licht *et al.*, 2011; Stuchlik, 2014; Takeuchi et al. 2014). Understanding the factors that permit appropriate and efficient rewiring is essential for understanding both developmental and neurodegenerative diseases.

Calcium is a key mediator of neuronal functions such as axonal growth, neurite protrusion, and spinogenesis (Clapham, 2007; Brini *et al.*, 2014). Previous studies have shown that spontaneous activity in neurons can result in a frequency-dependent rate of axon elongation that is inversely proportional to the frequency of calcium transients (Goldberg and Grabham, 1999; Gomez and Spitzer, 1999). The role of calcium in neurite growth and protrusions associated with development has been studied in different contexts (e.g., Mattson, 2007). This outgrowth process is stimulated by neurotrophic factors that carefully regulate the spatiotemporal aspects of intracellular calcium. Neurite growth can also be triggered by stress, pharmacological agents, or starvation (McKay *et al.*, 1999; Gilbert and Man, 2017). These factors may occur during disease states and contribute to inappropriate neurite growth, which can result in an

This article was published online ahead of print in MBoC in Press (http://www.molbiolcell.org/cgi/doi/10.1091/mbc.E19-09-0536) on December 11, 2019.

†These authors contributed equally to this work.

*Address correspondence to: Suzanne Scarlata (sfscarlata@wpi.edu); Padmini Rangamani (prangamani@ucsd.edu).

Abbreviations used: PI(4,5)P_2, phosphoinositol 4,5 bisphosphate; PLCβ, phospholipase Cβ.

increased number of smaller and nonproductive neurites, as seen in autism (Gilbert and Man, 2017).

Neurodegenerative diseases are associated with the disruption of normal calcium signaling. Specifically, diseases such as autism and amyotrophic lateral sclerosis (ALS) have been linked to overexcitation of neurons or excitotoxicity caused by abnormal calcium homeostasis (King *et al.*, 2016). However, the link between calcium homeostasis and the mechanical processes underlying neurite retraction remain poorly understood. Understanding the link between dysfunction of cellular calcium, especially prolonged signaling, and neuronal function is critical to understanding the mechanisms that underlie diseases typified by inappropriate neuronal excitation. While previous research has focused on the short-term effects of elevated cellular calcium after stimulation and its effects on neurite growth or on spontaneous spiking activity (Goldberg and Grabham, 1999; Gomez and Spitzer, 1999; Rosenberg and Spitzer, 2011), little is known about the effect of extended elevated calcium on these same neurites over time, that is, cases that mimic an extended overstimulated state. In this study, we investigate the effects of prolonged stimulation of the Gαq/PLCβ/PIP_2 /calcium signaling pathway by the neurotransmitter acetylcholine in a model neuronal cell line, PC12, and in the neuronal network in a small organism, *Caenorhabditis elegans*.

Calcium signals in neurites can be generated by several mechanisms. In synapses, postsynaptic cells receive an influx of calcium directly through the openings of transmembrane channels in response to neurotransmitter release (Voglis and Tavernarakis, 2006). Neurotransmitters, such as acetylcholine, activate G protein–coupled receptors (GPCRs) on the plasma membrane to cause the release of calcium from intracellular stores (McKay *et al.*, 1999). Furthermore, neurotropic factors activate receptor tyrosine kinases to increase intracellular calcium through another phospholipase C family, PLCγ. Downstream from these events is the opening of calcium-activated calcium channels on the endoplasmic reticulum (ER) membrane. Many of these channels are thought to respond to the increase in cytosolic calcium and to changes in the physical properties of the plasma membrane. These increases in cellular calcium regulate specific transcription factors and posttranscriptional processes that lead to appropriate downstream responses (West *et al.*, 2001).

In this study, we show that neurites will retract completely to the soma following extended stimulation of the GPCR/Gαq/PLCβ pathway. This pathway mediates signals from many hormones and neurotransmitters such as acetylcholine, dopamine, histamine, and melatonin (Kadamur and Ross, 2013). Signaling begins with ligand binding to its specific G protein–coupled receptor to activate the Gαq family of G proteins by exchange of GTP for GDP. The GTP-bound Gαq subunits then activate phospholipase Cβ (PLCβ). PLCβ catalyzes the hydrolysis of phosphatidylinositol 4,5-biphosphate (PIP_2) to inositol 1,4,5-triphosphate (IP_3) and diacylglycerol (DAG). IP_3 binds to receptors on the endoplasmic reticulum, allowing the release of calcium from intracellular stores into the cytoplasm. The elevated calcium can then change the activity of a variety of intracellular proteins to generate a specific cell response.

Incorporated into this pathway are a number of positive and negative feedback loops. The initial calcium release generated by PLCβ in turn stimulates the highly active PLCδ that synergizes the calcium response (Guo *et al.*, 2005). Increased calcium also opens calcium-induced calcium channels, further strengthening calcium responses (Lohmann and Wong, 2005). Negative feedback comes from the internalization of ligand-bound receptors into endosomes over a few minutes, which typically return unbound receptors to the plasma membrane over a period of 20–30 min (Freedman and Lefkowitz, 1996). Additionally, Gαq has GTPase activity that returns it to the basal state, and this activity is stimulated by the GTPase activating (GAP) activity of PLCβ (Berstein *et al.*, 1992), along with RGS proteins that quickly turn off the signal (Dohlman and Thorner, 1997). It is notable that these feedback loops are highly sensitive to the concentration of the pathway components and the concentrations of competing species, as well as the physical state of the plasma membrane, which drives aggregation of the ligand-bound receptor and internalization, the accessibility of $PI(4,5)P_2$ substrates to PLCβ and PLCδ, and the opening of calcium channels.

Components of the Gαq/PLCβ/$PI(4,5)P_2$ pathway are also involved in the regulation of membrane tension and cytoskeletal remodeling. The coupling between membrane tension and cytoskeletal adhesion through $PI(4,5)P_2$ was established nearly two decades ago by Sheetz and coworkers (Raucher *et al.*, 2000; Sheetz, 2001). In a series of elegant experiments, they showed that PIP_2 regulates cytoskeleton–plasma membrane adhesion (Raucher *et al.*, 2000) and that membrane tension plays a critical role in actin remodeling, membrane trafficking, and cell motility (van Rheenen and Jalink, 2002; Bittner and Holz, 2005; Diz-Munoz *et al.*, 2013). Subsequently, researchers continued to establish and identify increasing roles played by the plasma membrane tension and cortical tension in different cellular reorganization processes (Logan and Mandato, 2006; Rangamani *et al.*, 2011; Datar *et al.*, 2019). Specifically, in neurons, dynamics of growth cone formation, neurite protrusion, and axonal contractility have been shown to be mechanochemically coupled processes (Franze *et al.*, 2009; Kerstein *et al.*, 2015).

Despite these advances in neuronal biophysics, our understanding of synaptic rupture and neurite retraction remains incomplete, especially in terms of the mechanisms that underlie overexcitatory responses. In this study, we set out to investigate the effects of prolonged (i.e., several minutes) agonist stimulation of the Gαq signaling pathway in a model neuronal cell line (PC12). We find that prolonged stimulation results in tension-driven neurite retraction, unlike the behavior seen in shorter exposures to neurotransmitters. To understand the factors that underlie the observed neurite retraction, we followed the individual components during the process and developed a mathematical model to predict the effects of calcium stimulation by acetylcholine (ACh) and its extended response on retraction through mobilization of the pathways that impact neurite retraction.

Our predictive models showing that membrane tension and actin reorganization are coupled to calcium dynamics through Gαq/PLCβ/$PI(4,5)P_2$ were verified in cultured PC12 cells as well as in the neuronal network of the nematode *C. elegans*. The 302 neurons that comprise the nervous system of *C. elegans* (Sengupta and Samuel, 2009) have been well characterized, and these organisms have been used as models to understand neurite formation and retraction (Sengupta and Samuel, 2009). Because of its optical clarity, *C. elegans* allows us to monitor the effects of acetylcholine stimulation on synapses in real time by microscopy. We find that the *C. elegans* neural architecture exhibits the same retraction behavior when exposed to Gαq agonists showing rupture along the spine in the nerve ring, suggesting that the coupling between membrane tension and calcium dynamics occur on the organismal level. Taken together, our studies connect signaling processes with mechanical effects that allow us to predict the signaling conditions that shift from outgrowth and maintenance to retraction.

RESULTS

Prolonged exposure to carbachol causes neurite retraction

Cultured PC12 cells differentiate to a neuronal phenotype upon treatment with nerve growth factor (NGF), which initiates activation

through TrkA receptors (Greene and Tischler, 1976). This treatment results in growth of neurites from the cell body that extend to roughly three times the length of the body over a 36-h period. These neurites can then connect with neurites from other cells, resulting in long tubular structures (Drubin *et al.*, 1985).

Addition of a Gαq agonist to the cells activates PLCβ to catalyze the hydrolysis of $PI(4,5)P_2$. This hydrolysis releases $Ins(1,4,5)P_3$ into the cytosol, which then binds to $Ins(1,4,5)P_3$ receptors on the ER to release calcium from intracellular stores. In addition to eliciting calcium signals, $PI(4,5)P_2$ hydrolysis can exert mechanical effects on cells by altering membrane tension and actin–membrane adhesion (Raucher *et al.*, 2000; Sheetz, 2001; Logan and Mandato, 2006). We sought to understand the interactions between the Gαq/PLCβ pathway and mechanical features of membrane–actin interaction (Figure 1, A and B).

We found that when we added a Gαq agonist, such as carbachol or bradykinin, to PC12 cells, the well-formed neurites became thinner, their connections ruptured (compare Figure 1C with Figure 1E and Supplemental Figure S1), and they retract toward the soma after a period of 5–10 min (Figure 1, E and F). After retraction, the excess membrane appears as blebs around the sides of the cell (Figure 1G). This behavior was seen in every cell viewed in more than 100 experiments, but was not seen when a PLCβ inhibitor was added, or a Gαi agonist such as isoproterenol was used. The initiation and rate of retraction depended on the particular treatment and condition of the experiment, as described below. The extent of retraction in a specific time period was robust to the length and thickness of the neurite.

Neurite retraction is coupled with the Gαq/PLCβ/calcium pathway

We followed the activation of the Gαq/PLCβ/calcium signaling pathway upon stimulation in single PC12 cells using the fluorescent calcium indicator Calcium Green, to determine whether neurite retraction is concurrent with activation. Our approach was to follow some of the molecular constituents of the Gαq pathway and determine the temporal correlation between activation of the individual signal components and neurite retraction. The retraction velocities of a generic Gαq-coupled receptor (i.e., the bradykinin receptor type 2 or B2R) were measured by transfecting cells with a fluorescence-tagged construct and stimulating the cells with an agonist (i.e., bradykinin). We note that B2R is not endogenous to PC12 cells, thus allowing us to compare Gαq-associated retraction with that which results from stimulation of endogenous muscarinic receptors. We find retraction behavior for neurite retraction after stimulating the B2R transfected cells with bradykinin identical to that which results from carbachol stimulation (Figure 2). These results support a connection between neurite retraction and Gαq/PLCβ activation.

We calculated the velocity of neurite retraction by analyzing the decrease in length of each neurite at each time point during the experiment (see *Materials and Methods*). These velocities were analyzed for PC12 cells transfected with eCFP-B2R *(blue)* and for the plasma membrane *(orange)* as monitored by phase contrast imaging (Figure 2A). We find that the retraction of the plasma membrane is more gradual than that of the receptor, suggesting that movement of the receptor toward the soma precedes the membrane.

Activation of the PLCβ pathway through Gαq-GPCRs results in hydrolysis of the signaling lipid $PI(4,5)P_2$. We followed the change in the level and distribution of $PI(4,5)P_2$ of the plasma membrane surrounding the soma and neurite during retraction using a fluorescent $PI(4,5)P_2$ sensor (i.e., eGFP-PH-PLCδ1). Our data show that $PI(4,5)P_2$ moves from the neurite into the soma with a retraction velocity

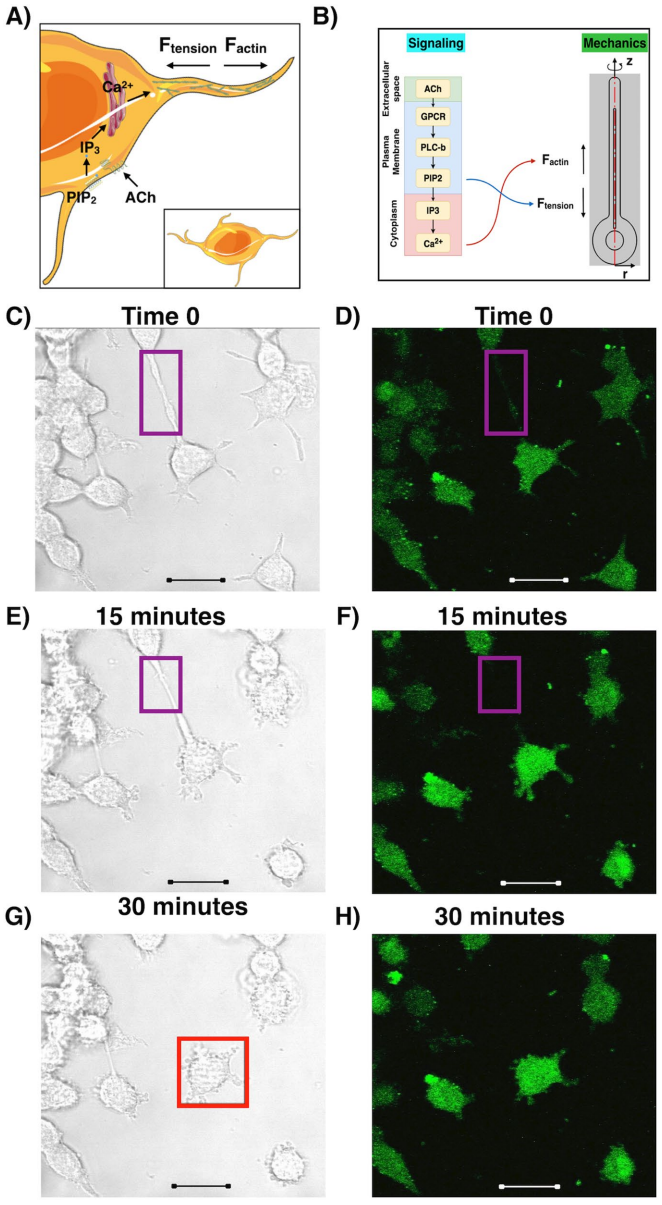

FIGURE 1: Neurite retraction in PC12 cells is induced by calcium stimulation. (A) Cartoon of the mechanochemical events underlying neurite retraction in a PC12 cell. The figure depicts the interconnection between calcium signaling and force regulation due to membrane cortical tension and actin remodeling. (B) Schematic showing the coupling between signaling and mechanical changes within the PC12 cell. We identify membrane cortical tension and actin dynamics as key players controlling neurite retraction rates and link calcium dynamics to actin reorganization and force generation, and $PI(4,5)P_2$ hydrolysis to membrane tension change and tension force generation. Using this coupled model, we are able to reproduce the neurite retraction behavior observed experimentally. (C, D) Sample images of differentiated PC12 cells before stimulation. Confocal phase contrast (C) and fluorescence images of cells loaded with a fluorescent calcium sensor, Calcium Green (D) are shown. (E–H) Stimulation of cells with carbachol results in neurite thinning, retraction, and synaptic rupture. At 15 min after the addition of carbachol, we observe membrane retraction (e.g., purple box) and thinning of the neurite (E, F). At 30 min after carbachol addition, we see a complete retraction of the neurites into the soma and membrane blebbing at the retraction sties (e.g., red box) (G, H). In all images, the scale bar is 20 μm. Identical behavior was seen in 20 cells.

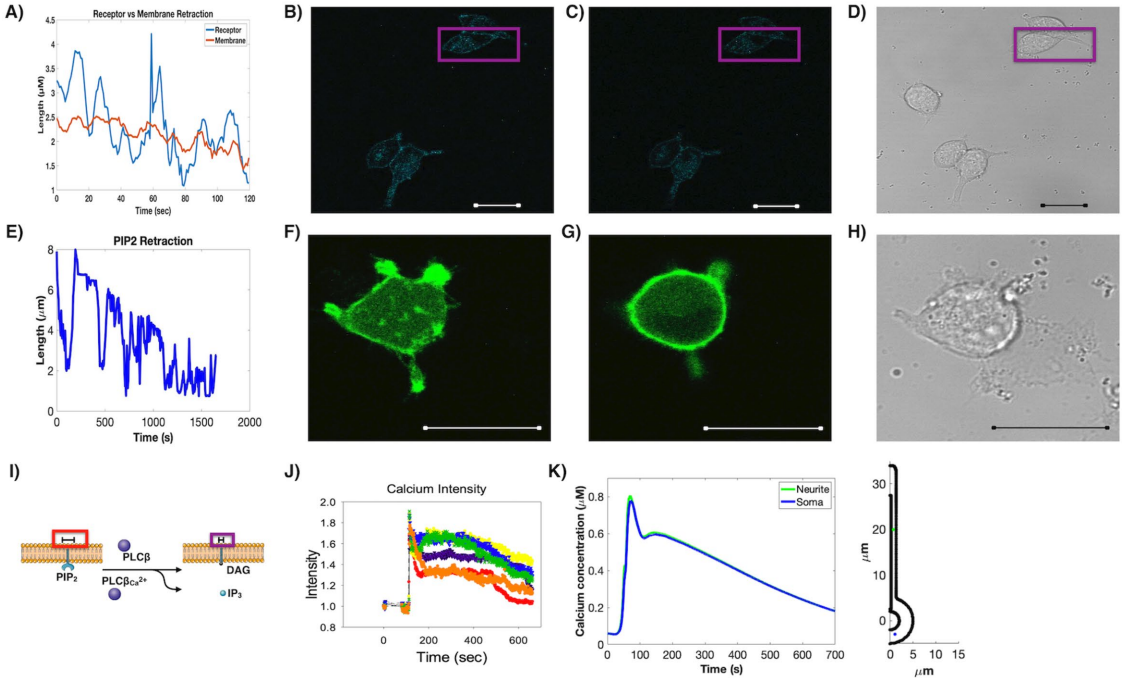

FIGURE 2: Neurite retraction of PC12 cells upon Gαq stimulation. (A) Decrease in neurite length of the B2R receptor in PC12 cells (blue) as compared with slow reduction in length of the membrane as followed by phase contrast (orange). (B) Images of differentiated PC12 cells expressing eCFP-B2R before stimulation with bradykinin and (C) 30 min after stimulation, where purple box shows the retraction data of A, and the corresponding phase contrast image is shown in D. (E) Decrease in neurite length as followed using a fluorescent PI(4,5)P_2 sensor, PH-PLCδ1 (Garcia et al., 1995), where distinct oscillations are seen. (F–H) Images of a differentiated PC12 cell expressing PH-PLCδ1 (F) before stimulation and (G) 30 min after stimulation with carbachol and (H) the corresponding phase contrast image. (I) Cartoon showing the hydrolysis of PI(4,5)P_2 to Ins(1,4,5)P_3 and DAG, depicting the larger head group of PIP_2, denoted by the scale bar (red box), as compared with the smaller DAG that remains in the membrane after hydrolysis (purple box). This decrease in the size of the membrane-bound molecule (PI(4,5)P_2 to DAG) leads to a local change in tension (denoted by the scale bars). IP_3 moves into the cytosol and the ER, causing a release of calcium. (J) Graph of calcium intensity in neurites of six different cells. This graph shows the lag time after the addition of carbachol, the initial spike in calcium, and the slow recovery. (K) Model replicating the intensity of calcium over time at two spatial locations (in the neurite and in the soma) after stimulation by carbachol. Inset: location of traces within the model geometry (in the neurite and in the soma). In all images, the scale bar is 20 μm, and $n > 15$ cells.

similar to that of the GPCR (Figure 2E). However, this movement is oscillatory, showing three precipitous drops and recoveries during the retraction event. These are three distinct movements of PI(4,5)P_2 during the observed retraction, which occur at similar times (~3, 10, and 15 min) for all cells tested and are interpreted as being due to PI(4,5)P_2 replenishment during the course of the retraction.

In general, Gαq activation produces an increase in calcium, typified by an initial spike in the first few minutes followed by a slow recovery. We followed the calcium behavior upon stimulation in single cells using Calcium Green (Figures 1, D, F, and H, and 2J). Correlating calcium responses with neurite retraction shows that retraction occurs even in this initial phase and continues through the duration of the recovery phase.

We constructed a spatial model of the Gαq/PLCβ/PI(4,5)P_2 signaling pathway using reaction–diffusion equations. The reactions, kinetic parameters, and diffusion constants are given in Tables S1–S4 in the Supplemental Material (SOM). The soma of the PC12 cell was modeled as a simplified geometry capturing the key features of these cells. Briefly, the soma was modeled as a sphere with a radius of 5 μm, and the neurite was modeled as a cylinder with a radius of 1.25 μm and a length of 30 μm. The endoplasmic reticulum was modeled as a cylinder with a radius of 0.25 μm and a length of 25 μm, and the nucleus as a sphere with a radius of 2 μm. Geometric details are given in Supplemental Table S5. The nucleus was treated as an excluded volume, while the ER was treated as a calcium source. Computational modeling of this pathway in a three-dimensional spatial model using finite elements captured the calcium transients with the same time scale as the experiments (compare Figure 2, J and K). This framework sets the stage for the mechanical coupling of calcium dynamics to neurite retraction.

Actin remodeling proteins affect the dynamics of neurite retraction

Actin filaments are the major cytoskeletal components of synapses and are the key modulators of neurite plasticity. An actin filament is a dynamic structure in which monomers disassemble from one end and reassemble on the other, a behavior known as molecular treadmilling. Retraction involves inward movement of the actin structure that defines the neurite shape, and so any model of retraction must incorporate actin disassembly. In neurites, actin filament remodeling is known to be associated with the drag forces related to protrusion (Datar *et al.*, 2019). Additionally, PI(4,5)P_2 hydrolysis is closely connected to membrane-actin adhesion and membrane tension regulation (Raucher *et al.*, 2000).

On the basis of our experimental observations (Figure 2), we coupled PI(4,5)P_2 hydrolysis and calcium release following carbachol

stimulation with a mechanical model that balances the forces due to actin depolymerization and membrane cortical tension change. Owing to the time-scale separation between the biochemical signaling dynamics and neurite retraction, we coupled the three-dimensional spatial model of the Gαq/PLCβ/calcium signaling pathway (Figure I, A and B) to an ordinary differential equation model of neurite mechanics, assuming uniform signaling dynamics at extended timescales (Section S1-2 in the SOM). Briefly, the mechanical model proposes a force balance acting on the tip of the neurite (Hassinger *et al.*, 2017). The force due to the actin cytoskeleton is acting outward, away from the soma, and the force exerted by the membrane cortical tension is acting toward the soma. In this case, we assume that the cortical tension is a function of the change in the area of the membrane. This change in membrane area can result from PI(4,5)P_2 hydrolysis (Sheetz and Dai, 1996; Raucher *et al.*, 2000), from endocytosis of GPCRs (Getz *et al.*, 2019), and from changes in tension (Simunovic *et al.*, 2017). The force exerted by the actin cytoskeleton is modeled phenomenologically as a function of calcium-mediated cofilin and retrograde flow (Bornschlogl *et al.*, 2013). Thus, the net force balance can be written as

$$\underbrace{-F_{\text{tension}}}_{\text{force due to cortical membrane tension}} + \underbrace{F_{\text{actin}}}_{\text{force due to actin dynamics}} = \underbrace{\frac{\eta}{k_L L}\frac{dL}{dt}}_{\text{drag forces}} \quad (1)$$

where

$$\eta = \underbrace{\mu_e}_{\text{drag coefficient for external fluid}} + \underbrace{\frac{\mu_m}{\delta}}_{\text{drag coefficient for membrane}} \quad (2)$$

Modeling the neurite as a cylinder with a hemispherical end cap, we obtain the governing equation for the length of the neurite as

$$\underbrace{\frac{dL}{dt}}_{\text{rate of change of neurite length}} = \underbrace{\frac{k_L L}{\eta}}_{\text{drag coefficients and length effects}} \underbrace{\left(-F_{\text{tension}} + F_{\text{actin}}\right)}_{\text{forces}} \quad (3)$$

This governing equation combines the force balance above with experimental observations that retraction velocity is proportional to neurite length. The force due to membrane cortical tension and actin dynamics depends on equations for τ and F_{actin}, respectively, given as

$$\frac{d\tau}{dt} = \underbrace{\frac{d\text{Area}}{dt}\left(f(\text{PIP}_2)\right)}_{\text{area change with PIP2 dependence}} \underbrace{F_{\text{perPIP}_2}}_{\text{tension change per PIP2}} \underbrace{\frac{k_{\text{tension}}}{A_0}}_{\text{unit correction}} \quad (4)$$

and

$$\frac{dF_{\text{actin}}}{dt} = \underbrace{\frac{F_{\text{per Actin}} k_{\text{actin}}}{L_0}}_{\text{force and length effects}} \underbrace{\left(k_{\text{const}} + k_{\text{cofilin}} + k_{\text{actin}} + k_{\text{drebrin}}\right)}_{\text{k contributions}} \frac{dL}{dt} \quad (5)$$

This is a phenomenological model with a combination of parameters from literature and constants fit to the experimental results (see SOM). In particular, Eqs. 4 and 5 depend on *f*(PIP2) and *g*(CofilinAct), which are sigmoidal functions that trigger in response to PI(4,5)P_2 and activated cofilin, respectively (Zmurchok *et al.*, 2018).

Using this model, we simulated calcium-mediated neurite retraction in control cells. We found that the model is able to capture the dynamics of neurite retraction events (Figure 3C). These models utilized experimental retraction data collected using differentiated PC12 cells transfected with small amounts of mCherry-actin to fit the phenomenological constants (Figure 3). Effectively, the model predicts that when the force exerted by actin is matched by the force due to tension, there is no change in the length of the neurite. Upon increase in PI(4,5)P_2 hydrolysis and calcium release into the cytosol, the forces due to membrane cortical tension increase, while the forces exerted by the actin decrease, and the neurite pulls back.

If this prediction is true, then we should be able to alter neurite retraction behavior by altering the expression of actin-related proteins or membrane tension separately. We next probed neurite retraction dynamics by varying the concentration of select

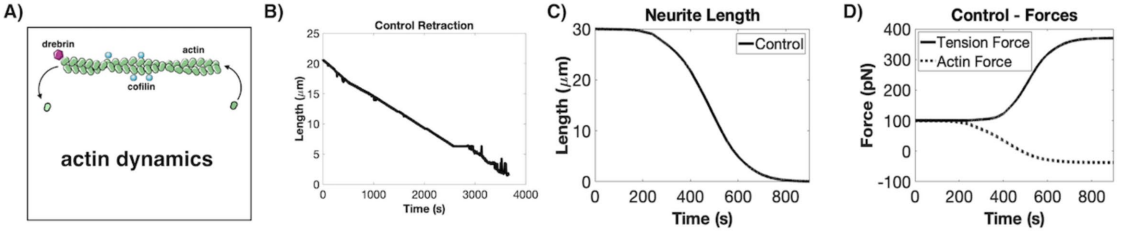

E)

Retraction Start Times of Control Cells	
Neurite 1	2.2 minutes
Neurite 2	2.4 minutes
Neurite 3	8.0 minutes
Neurite 4	7.8 minutes
Neurite 5	2.6 minutes
Neurite 6	4.0 minutes
Neurite 7	4.2 minutes
Neurite 8	2.5 minutes

FIGURE 3: Modeling of neurite retraction. (A) Simplified schematic of actin dynamics depicting assembly/disassembly as a combination of effects due to actin, cofilin, and drebrin concentration. (B) Example of retraction in response to carbachol stimulation of differentiated PC12 cells transfected with mCherry-actin. Identical behavior was seen over an average of eight neurites shown in E. (C) Computational results for neurite retraction determined from the described model. (D) Calculation of force plots due to increased tension in response to PI(4,5)P_2 hydrolysis, internalization of ligand-bound GPCRs, and tension effects. The force due to actin decreases and switches direction in response to actin breakdown and retrograde flow. (E) Table showing variation of retraction times under the same conditions.

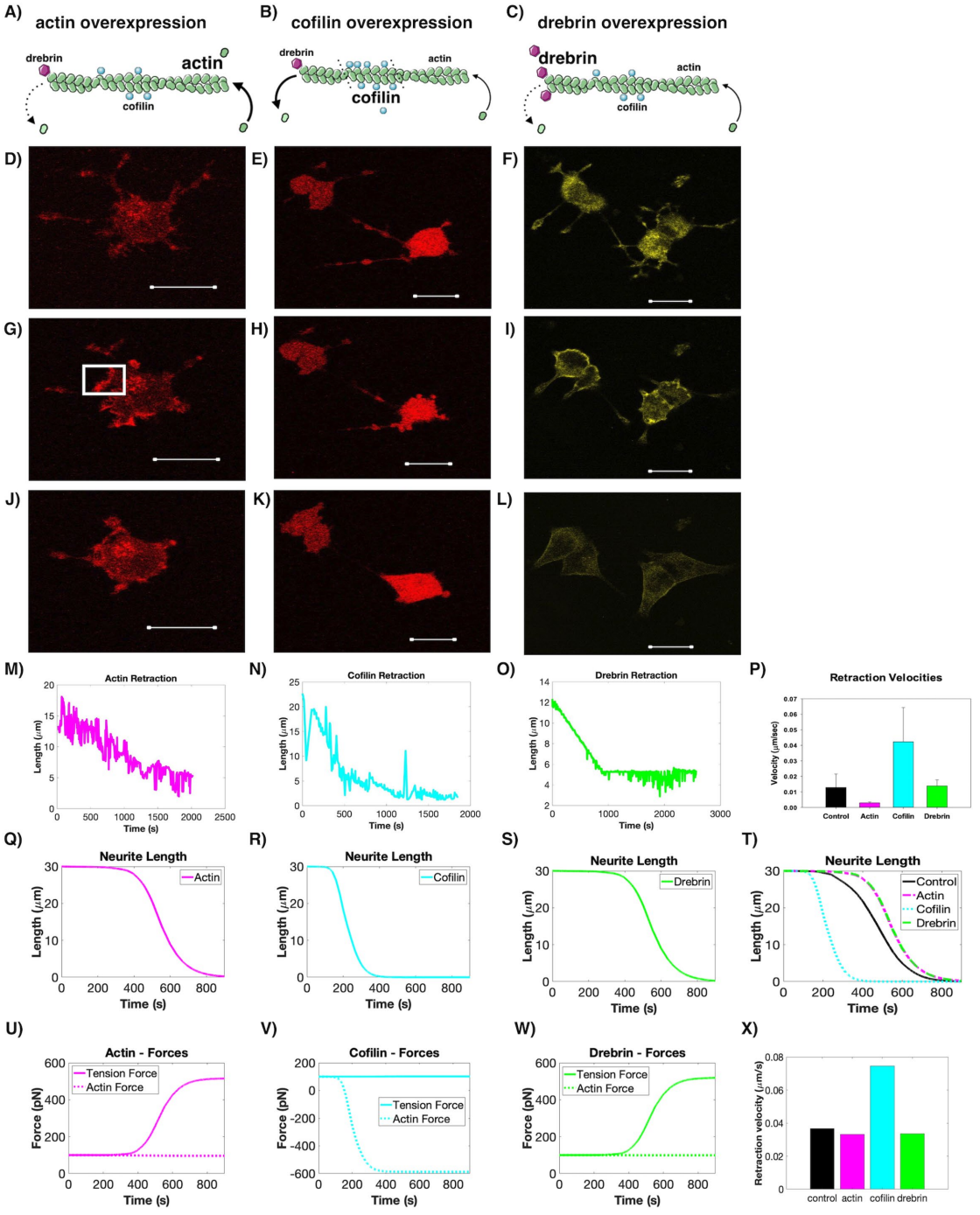

FIGURE 4: Experimental validation of model predictions. (A–C) Schematic of the experimental study to test the actin force model where mCherry-actin, mCherry-cofilin, or eYFP-Drebrin was expressed at varying levels in PC12 cells using increasing amounts of DNA in the transfections. The corresponding images are shown directly below. While cofilin activity is mediated by calcium, actin and drebrin dynamics depends on local concentrations. Column 1 (panels A, D, G, J, M, Q, U) is results from studies following mCherry-actin expressed in PC12 cells. The increase in actin, as estimated by Western blotting, reduces the change in the actin force. Panel D is an example image of cells before carbachol stimulation. G is 15 min poststimulation, showing the beginning stage of actin breakdown, indicated by the white box, and J is 30 min poststimulation. A representative retraction velocity curve is shown in M. Panels Q and U are the results of modeling the retraction velocity (Q) due to a tension force and an actin force (U). We note that the overexpression of actin leads to less of a decrease in actin force, since the increased actin concentration slows overall actin breakdown. Column 2 (panels B, E, H, K, N, R, V) shows how cofilin overexpression creates a large negative actin force to increase the rate of disassembly as shown in the schematic B. Panel E is an example image of cells expressing cofilin-RFP before carbachol stimulation, H is 7 min poststimulation, and K is 16 min poststimulation. A representative retraction velocity curve is shown in N. Panels R and V are the results of modeling the retraction velocity (R) due to the tension force and a larger negative actin force (V) since increased cofilin concentration increases actin breakdown. Column 3 (panels C, F, I, L, O, S, W) shows how drebrin overexpression slows the change in actin force as shown in

actin-related proteins such as cofilin, drebrin, and actin itself, both in experiments and in modeling.

Actin modulators regulate neurite retraction velocity

We followed actin disassembly in real time during carbachol-stimulated retraction using mCherry-actin in control cells and cells overexpressing cofilin or drebrin (Figure 4). Cofilin increases severing of actin filaments, increasing actin filament breakdown, while drebrin stabilizes actin filaments, inhibiting disassembly (McCullough *et al.*, 2008; Mikati *et al.*, 2013; Calabrese *et al.*, 2014; Grintsevich and Reisler, 2014). Figure 4, D–L, shows screen shots of the time lapse video made during retraction: Figure 4, D–F, shows representative cells before stimulation with carbachol, Figure 4, G–I, shows the same cells at the beginning of retraction, and Figure 4, J–L, shows the cells at longer times. Movies of retraction (SOM2*)* were analyzed to obtain the retraction velocities under the three different conditions (Figure 4, M–P). This quantification enables the comparison of the neurite retraction dynamics of actin in our controls versus actin when cofilin and drebrin are overexpressed. As expected, overexpression of cofilin enhances the rate of neurite retraction (Figure 4, M vs. N), and complete retraction results in cells with a trapezoidal morphology rather than the circular one typifying undifferentiated PC12 cells. This altered morphology likely stems from the smaller number of actin filaments throughout the cell due to cofilin overexpression (Pavlov *et al.*, 2007).

We expected that transfection of the cells with drebrin would strongly impede neurite retraction in the presence of carbachol, because drebrin is known to bind assembled actin filaments (F-actin) and stabilize them (Sharma *et al.*, 2011; Mikati *et al.*, 2013; Nair *et al.*, 2017). Small amounts of actin allowed a sustained linear decrease (Figure 4O) whose compiled average was within error of mCherry-actin alone (Figure 4P). These data support the idea that disruption of the intact actin network and its dynamic modeling when impeded by cofilin overexpression (increased severing) or by drebrin overexpression (inhibition of disassembly and remodeling) are key driving forces in governing retraction dynamics.

We modeled overexpression of cofilin, drebrin, and actin in the mechanical framework by altering the F_{actin} terms (Eq. 5) to represent the known effects of these proteins through the k contributions for each protein. We modeled actin force overall as a stress–strain relationship, where the k terms captured the contribution of each protein to overall actin force dynamics. For example, cofilin expression was incorporated into our constitutive equation as an increase in the total cofilin available for calcium activation, which therefore caused a faster decrease in F_{actin} by increasing the magnitude of the rate of change of F_{actin} through the $k_{cofilin}$ term. As a result, our model predicts that neurite retraction velocity is higher for cofilin overexpression than for controls (Figure 4, R and V). Similarly, we modeled drebrin overexpression by increasing drebrin concentration within the $k_{drebrin}$ term, consistent with experimental observations that a higher drebrin concentration slows actin depolymerization and thus slows the decrease in F_{actin} (Sharma *et al.*, 2011; Mikati *et al.*, 2013). Therefore, our model predicts that drebrin overexpression slows neurite retraction velocity relative to that in controls (Figure 4, S and W). Actin overexpression can be modeled in a similar manner to that of drebrin and is captured through the k_{actin} term. Thus, increasing actin concentration is essentially increasing the actin-to-cofilin ratio and therefore slowing the decrease in F_{actin}. Our model predicts that actin overexpression will slow neurite retraction velocities from those for controls (Figure 4, Q and U).

The results in Figure 4 show that by varying cofilin, drebrin, and actin concentrations, we predict different actin force dynamics that translate to different neurite retraction rates. Specifically, we predict that cofilin, actin, and drebrin overexpression leads to more rapid, slower, and slightly slower neurite retraction velocities than in controls, respectively. Our modeling results agree with experimental observations and suggest that actin disassembly and inhibition of reassembly are necessary for retraction. To support these studies, we quantified experiments that measured retraction of control cells and cells that overexpressed actin, cofilin, and drebrin. The experimental velocities of the retractions are plotted in Figure 4P and validate our model predictions in Figure 4X.

Neurite retraction can be driven by membrane tension.

Given that there are two contributions to the force acting on the neurite, one from actin and the other from membrane cortical tension, we next asked whether neurite retraction could be driven by changes to the membrane cortical tension alone. We directly tested this idea using hyperosmotic stress to increase membrane tension. Increasing the hyperosmotic stress from 300 to 600 mOsm on cultured PC12 cells resulted in the same retraction behavior and time scale as seen with carbachol stimulation (Figure 5A). To determine the change in membrane tension induced by this change in osmolarity, we measured tension by atomic force microscopy (AFM). This method allowed us to assess the stiffness of cells by measuring the amount of deflection experienced by a cantilever with a known spring constant as it indented the surface of the cell. For undifferentiated, differentiated, and retracted PC12 cells, AFM measurements were taken at the bases of the neurites or retracted neurites. The stiffness of each cell was determined by averaging the stiffness values at three separate locations on each cell in order to combat the inherent heterogeneity in cell structure while ensuring no localized damage from a previous measurement. Undifferentiated cells were the stiffest condition tested, followed by retracted and then differentiated (Figure 5B).

We also used AFM to determine the stiffness of cells subjected to hypoosmotic and hyperosmotic stress for undifferenced and differentiated PC12 cells. Hypoosmotic and hyperosmotic stress, which lead to cell swelling and cell dehydration, respectively, result in an increase and a decrease in cell stiffness, respectively (Figure 5B). Force curves that are representative of the average stiffness value for each condition show a smooth Hertz model relationship between indentation depth and applied force, as expected (Figure 5, C and D). Taken together, these studies show a direct correlation between cell stiffness and osmotic stress, which is also correlated with retraction.

schematic C. Panel F is an example image of cells expressing drebrin-eYFP before carbachol stimulation. I is 15 min poststimulation, and L is 30 min poststimulation. A representative retraction velocity curve is shown in O.
A representative retraction velocity curve is shown in O. Panels S and W are the results of modeling the retraction velocity (S) due to the tension force and the actin force (W). We note that increased drebrin concentration resists actin breakdown. Panels P, T, and X are compiled retraction velocities obtained experimentally (P) control ($n = 4$), actin ($n = 4$), cofilin ($n = 3$), and drebrin ($n = 4$) showing standard error, and computationally (T) and (X), showing the very close correlation between experimental and theoretical results. All scale bars = 20 μm.

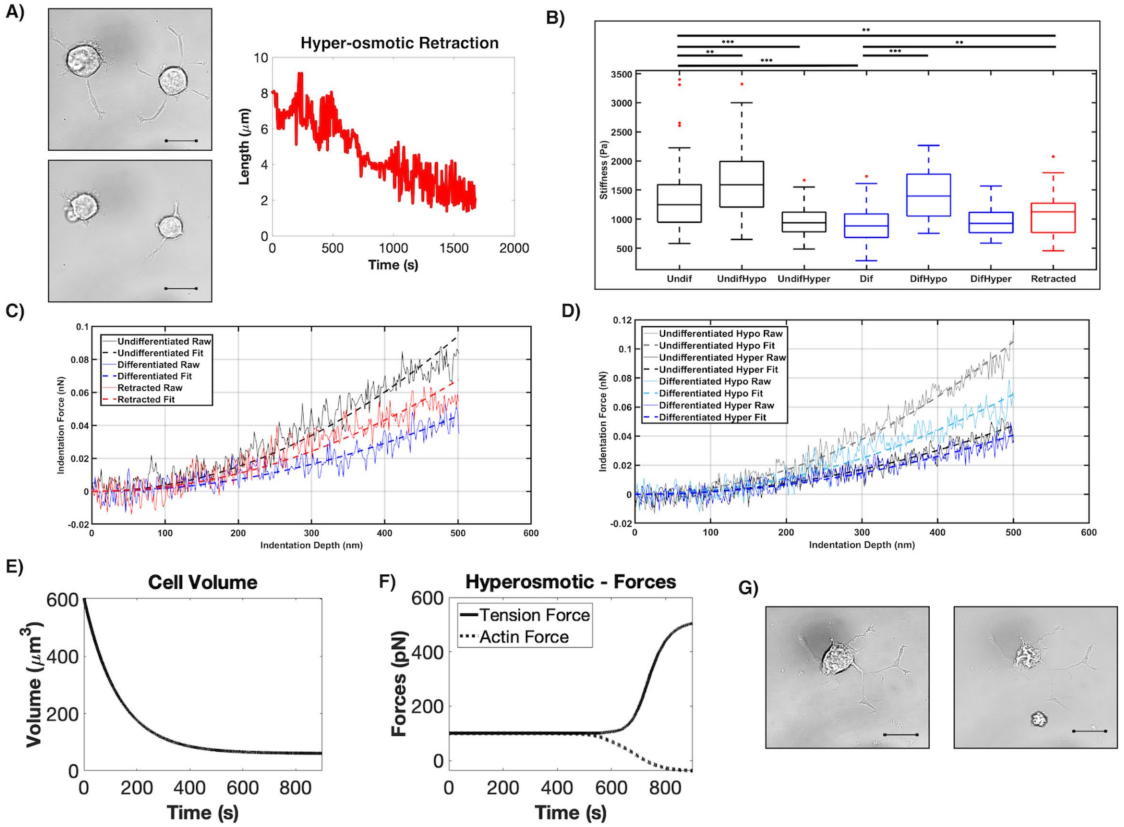

FIGURE 5: Neurite retraction can be induced by membrane tension in response to hyperosmotic stress. (A) Phase contrast images of PC12 cells under isotonic conditions (300 mOsm, top left) and hyperosmotic conditions (450 mOsm, bottom left) after 10 min. The corresponding neurite retraction curve for the cell on the left is shown to the right. (B) Cell stiffness as measured by atomic force microscopy of undifferentiated and differentiated PC12 cells under isotonic conditions and cells subjected to hypoosmotic (150 mOsm) or hyperosmotic (450 mOsm) stress, where the number of cells $n = 14–46$, and where $^{**}p < 0.01$, $^{***}p < 0.001$. (C, D) Force curves representative of the average stiffness values in B with automated Hertz model fitting (see methods) over 500 nm indentation for untreated cells (left) and hypoosmotic/hyperosmotic treated cells (right). (E, F) Hyperosmotic stress is modeled as an instantaneous increase in membrane tension due to the reduction in volume–to–surface area ratio, which causes a membrane tension increase and a smaller cytoskeletal force (E) and triggers neurite retraction through an increase in primary tension force (F), in the absence of ligand input. (G) Phase contrast images of differentiated PC12 cells before the application of osmotic stress (left) and after increasing the osmolarity from 300 to 600 mOsm in calcium-free medium. Note the loss in cell volume seen by membrane puckering but without retraction (right)

Within our model, we can also probe neurite retraction dynamics by varying the contribution of tension, the τ component of the mechanical model. Membrane cortical tension is altered under hyperosmotic conditions when water expulsion from the cell leads to a reduction in volume–to–surface area ratio. Therefore, to model hyperosmotic conditions instead of a carbachol stimulus, we predict that this volume–to–surface area ratio change causes an increase in membrane cortical tension. Therefore, we model a slightly elevated membrane cortical tension initial condition that triggers a related force (Figure 5E) and neurite retraction (Figure 5F). We also see a change in actin force, triggered by the coupling between actin and tension in the model, which is also predicted experimentally due to the necessary actin reorganization during retraction caused by hyperosmotic conditions. Therefore, our model predicts neurite retraction in the absence of a ligand stimulus with hyperosmotic conditions (Figure 5F), indicating that membrane cortical tension is a key component governing neurite retraction dynamics.

We tested whether the retraction that results from osmotic stress is convergent with the Gαq/PLCβ pathway. Keeping in mind that membrane compression regulates calcium flux to drive actin dynamics in model systems (Hartzell *et al.*, 2016; Nourse and Pathak, 2017; He *et al.*, 2018), we determined whether hyperosmotic stress would open calcium channels to allow divalent cation influx to relieve the osmotic stress. Using a fluorescent calcium indicator, we found that increasing the osmotic strength from 300 to 600 mOsm resulted in a small increase in intracellular calcium by ~10% of the increase seen for ACh stimulation. To verify that calcium is mediating retraction, we removed extracellular calcium from the media and found that even though increasing the osmotic strength through the addition of KCl caused membrane folds and puckering, consistent with a loss in cell volume, neurite length remained constant (Figure 5G). This result indicates that the two types of retraction pathways converge on calcium levels, those initiated by Gαq/PLCβ stimulation and those initiated by extracellular calcium influx by tension-sensitive calcium channels.

Prolonged exposure to Gαq agonists leads to nerve ring disruption in *Caenorhabditis elegans*

To determine whether we could disrupt neuronal connections and retract neurites in a neuronal network, we used the optically clear

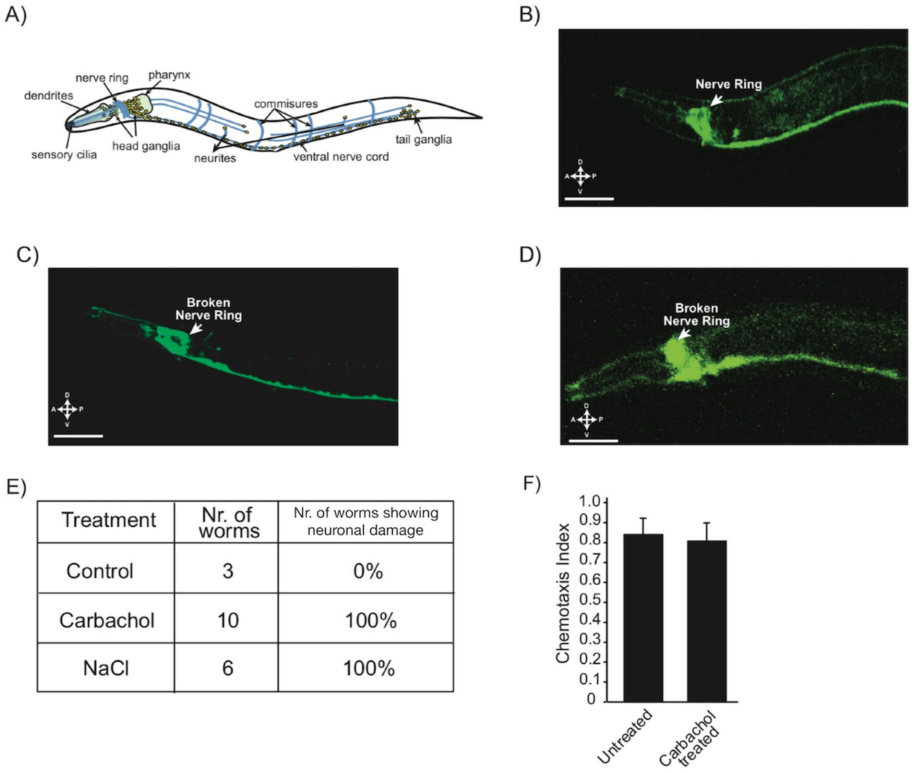

E)

Treatment	Nr. of worms	Nr. of worms showing neuronal damage
Control	3	0%
Carbachol	10	100%
NaCl	6	100%

FIGURE 6: Neurite retraction induced by membrane tension is seen in the neural network of *C. elegans*. (A) General schematic of the nervous system of *C. elegans*. (B) Untreated *C. elegans* that expresses GFP G-CAMP through the nerve ring and ventral nerve. (C) A representative worm with 1 mM carbachol for 30 min showing a broken nerve ring and pilling ventral nerve. (D) A representative worm subjected to hyperosmotic stress showing a broken nerve ring. (E) Table showing the compiled results of each experimental condition and the number of resulting nerve rings that were broken. (F) Results of a chemotaxis assay testing movement of *C. elegans* with and without l mM carbachol treatment.

model system C. *elegans*. We first used a strain of *C. elegans* (QWl166) that expresses an integrated fluorescent calcium sensor G-CaMP throughout the nervous system. This system allows us to visualize by fluorescence the neurons that show increased calcium levels in response to acetylcholine stimulation. This specific strain has fluorescence in every neuron in the nerve ring, allowing us to look at the ring as a whole, as well as fluorescence in the entire ventral nerve of the worm, which extends the entire length of the worm. We focused on acetylcholine signals emanating from neurons within the nerve ring located in the head of the worm and along the ventral nerve cord (Figure 6A). Normal signal transmission can be seen in the images in Figure 6B. For these studies, we wished to determine only whether there is broad neuronal rupture and retraction within the nerve ring and along the ventral nerve, which would be indicated by the lack of fluorescence in the center in the ring and dark spots along the ventral nerve. In every worm tested ($n = 10$), we find neuronal rupture with acetylcholine stimulation that occurs in the nerve ring close to the organism's mouth (Figure 6C). Additionally, we see a distinct pilling of the ventral nerve, which displays thinning and clustering, and portions that are no longer fluorescent, indicating large-scale neuronal damage.

We confirmed the connection between neuronal network disruption produced by extended acetylcholine stimulation to membrane tension by subjecting the worms to hyperosmotic stress (increasing the salt solution concentration by 50%). After osmotic stress, these organisms showed a lack of fluorescence in the nerve ring, indicating rupture and retraction of neurons. Also, we see much larger segments of the ventral nerve that have been disrupted with less pilling than seen for acetylcholine stimulation (Figure 6D). The somewhat different morphological effects on the ventral nerve seen in osmotic stress are most likely due to the ability of the stress to be distributed uniformly along the length of the organism, as opposed to carbachol, whose receptors are concentrated mostly in the mouth.

To support neuronal disruption of the worms by acetylcholine, we followed changes in movement of the whole organisms, using a chemotaxis assay with and without acetylcholine stimulation. These studies were also done using the *C. elegans* QWl166 strain. We see that after treatment with acetylcholine, 83% of the worms moved toward the attractant, while the remaining 17% did not move at all (Figure 6F).

DISCUSSION

For an organism to learn, neurons must break and reform connections with neighboring neurons, and disruptions in these processes underlie learning-based neurological diseases and neurodegeneration. Despite the importance of synapse severing and formation, the mechanisms that underlie neural plasticity are not well understood (Licht *et al.*, 2011). Previous studies of neural plasticity have mainly focused on contributors to neurogenesis in hippocampal neurons and cultured *Drosophila* neurons, such as neuronal stem cells (LaFerla, 2002). Here, we have defined the synaptic breakage and neurite rupture in neural plasticity in terms of membrane tension and calcium-induced retraction that will allow for predictable actin remodeling.

Calcium is a crucial component for the growth, differentiation, and survival of neurons (Rosenberg and Spitzer, 2011). Calcium helps to regulate the differentiation of specific neuronal types as well as their migration through the body, and calcium levels are directly liked to neurodegenerative diseases such as Alzheimer's (LaFerla, 2002). We followed neuronal cell response to extended calcium signals that may mimic dysfunctional states. Unexpectedly, we found that extended calcium levels resulted in complete neurite retraction, and this retraction can be seen by following the plasma membrane, by a GPCR coupled to Gαq, and by $PI(4,5)P_2$. These data show that the Gαq signaling pathways are intimately involved with the mechanical properties of the cell.

The connection between calcium signals from GPCR/Gαq and cell mechanics was supported using fluorescence-tagged actin and by measuring retraction when overexpressing cofilin, an actin depolymerizing protein, or drebrin, an actin monomer recruitment protein. Overexpressing cofilin at a level 6x higher than endogenous levels allows for much faster velocities of neurite retraction initiated by GPCR-Gαq/Ca^{2+} after an initial lag period. These observations correlate well with cofilin's ability to depolymerize actin, but shows that activation of the Gαq/$PI(4,5)P_2$/Ca^{2+} pathway is a necessary prerequisite. In contrast, cells

overexpressing drebrin show a similar retraction rate as endogenous which correlates to its ability to stabilize actin monomers (Mikati *et al.*, 2013). This observation indicates that the behavior we are viewing is due solely to actin depolymerization without contributions of the polymerization events. Thus, while Ca^{2+} signals drive retraction, actin plays a passive role.

There are other physiological events that might play a role in neurite retraction. PLCβ is the primary effector of Gαq, but we also note Gαq activates proteins that impact RhoA (see Sanchez-Fernandez *et al.*, 2014) potentially contributing to the mechanical changes associated with retraction. However, this contribution will be operative only for retraction that occurs in response to carbachol and not osmotic stress. Additionally, the loss of neurites during retraction shifts its associated plasma membrane population to the cytosol in the cell body. This net increase in the cytosolic PLCβ population will promote PLCβ's cytosolic roles in directing translation of specific mRNAs (see Scarlata *et al.*, 2018; Scarlata, 2019), which are typically not operative during Gαq stimulation. The net effect of cytosolic PLCβ would be shifting protein populations during longer times not probed in this study.

The coupling between calcium signaling and mechanical forces has been observed in cell motility and in dendritic spines during long-term potentiation, astrocyte calcium signaling, and neurite protrusion and formation (Mutalik *et al.*, 2018). On the basis of these studies, we postulated that neurite retraction results from changes in cortical tension brought about by receptor endocytosis, $PI(4,5)P_2$ hydrolysis and IP_3 generation, and an increase in intracellular calcium, and we formulated a mechanochemical pathway to test this idea. We found that, indeed, a force balance between cortical tension and actin-mediated forces, both of which are mediated by intracellular calcium levels, is sufficient to capture the dynamics of neurite retraction. This idea was explicitly tested by measuring changes in membrane stiffness with osmotic strength and by altering the effects of different actin remodeling proteins. We also found that the effects of actin and cortical tension could be uncoupled to a certain extent, pointing toward multiple mechanical pathways that could exquisitely regulate neurite retraction. We acknowledge that the proposed model is phenomenological, and while it captures the key physics of the processes underlying neurite retraction, future studies will focus on elaborating on some of the phenomenological relationships proposed here.

Our results show that acetylcholine-induced calcium signals may have a dramatic impact on neuronal morphology and synaptic connections, and this idea was demonstrated in *C. elegans*. Neurite formation and extension is essential to transition from neuroblast to mature neuron and *C. elegans* are an excellent model system to understand neurite formation and retraction. The site of nascent neurite outgrowth is determined by cell intrinsic factors that orchestrate the localized regulation of actin and microtubules, and in developing neurons, these factors are polarized at sites of neurite outgrowth in response to extracellular cues (Randlett, 2011). Our finding that the neural network of this organism can be modified by Gαq activation or increased mechanical tension may form a basis for studies that better describe neural rewiring paradigms.

In summary, our studies indicate the role of acetylcholine in facilitating neurite retraction. Further research on how this pathway interacts with other pathways to coordinate remodeling with such spatiotemporal precision will provide insights into the molecular basis of neurodegeneration.

MATERIALS AND METHODS

Cell culture, transfection, and differentiation

PC12 cells, which are derived from rat pheochromocytoma (ATCC CRL-1721), were cultured in 35-mm or 100-mm poly-D-lysine–coated Petri dishes using DMEM (Life Technologies) with 10% heat-inactivated horse serum (Life Technologies), 5% fetal bovine serum (Atlanta Biologicals), and 1% penicillin/streptomycin. The dishes were incubated with 5% CO_2 at 37°C. Cells were transfected using different amounts of plasmid based on the concentration as tested using a NanoDrop. Cells were transfected using Lipofectamine 3000 (Invitrogen) following the protocol of the manufacturer. The medium used in transfection was the same DMEM culture medium, with the exception of antibiotics to increase transfection efficiency, and the medium was changed back to normal culture medium after 24 h. Cells were differentiated using media that contained DMEM, 1% heat-inactivated horse serum, and 1% penicillin/streptomycin. Added to this would be a 1:1000 ratio of l00 ng/μl nerve growth factor (NGF) (Novoprotein). This medium is added to the cells for at least 48 h and up to 96 h to achieve long neurites.

Plasmids and maxi/min prep

Fluorescence-tagged plasmids were obtained and maxi/min prepped using a Qiagen kit and following the manufacturer's guidelines. The plasmids were obtained from Addgene. Actin #54967 was derived by Michael Davidson at Harvard Medical School, Drebrin #40359 was derived by Phillip Gordon-Weeks at King's College of London, Cofilin #51279 was derived by James Bamburg at Colorado State University, the Pleckstrin homology (PH)-domain of PLC8 #21179 was derived by Tobias Meyer at Stanford University, and the bradykinin type 2 receptor was modified from a construct provided by Fredrik Leed-Lundber, University of Texas, San Antonio.

Calcium green staining

Prior to imaging, cells were washed with Hanks' balanced salt solution (HBSS) with calcium, magnesium, no phenol red (Thermofisher), and then a 1:200 mixture of HBSS and Calcium Green (Thermofisher) was added and allowed to incubate for 1 h before imaging.

Preparation of carbachol

Carbachol in powdered form was obtained from Sigma Aldrich. It was dissolved in water to a final concentration of l mM at a volume of l0 ml and aliquoted into 500-μl portions to be used for each experiment. The solutions were kept at –20°C.

Fluorescence microscopy/stimulation of cells

Fluorescence imaging was done using a Zeiss LSM510 inverted confocal microscope. Imaging was carried out at least 48 h after transfection and differentiation. The cells were grown and imaged in a MAT-Tek 8 chamber glass-bottom plate or a MAT-Tek 35-mm glass-bottom dish. Once a single cell was found visually that expressed the plasmid or stain, the microscope was switched to the correct wavelength and laser intensity. A time series image was then started and stopped after 10 frames, the cells was manually stimulated by adding carbachol to the dish to achieve the desired final molarity, and the time series video was then started immediately after carbachol was added. Retraction velocities were determined by the software *Re-Track* (unpublished data).

Osmotic stress and EDTA studies

Osmotic stress studies were done using calcium-free isotonic media for imaging, with the addition of KCl at different concentrations to achieve osmotic stress. In studies that include EDTA (J.T. Baker),

cells were osmotically stressed and EDTA was added to the dish to give a final concentration of 0.5 µM for partial neurite retraction and 1 µM for full neurite retraction.

Plasmid-specific studies

Calcium Green and enhanced green fluorescent protein (eGFP) studies were imaged using an argon laser at 488 nm. Red fluorescent protein (RFP) and mCherry were imaged using argon ion and HeNe lasers at 543 nm. YFP and CFP were imaged using argon ion and HeNe lasers at a wavelength of 545 nm. Multitrack imaging can also be done combining of these setups. Images were taken by alternating between probes when data for more than one were being monitored, and these images were subsequently merged.

Atomic force microscopy stiffness measurements

Live cells were probed utilizing an MFP-3D-BIO atomic force microscope (Asylum Research) and a DNP cantilever (Bruker) with nominal spring constant 0.06 N/m. The cantilever was calibrated before each measurement to ensure accuracy. Cells were seeded on 60 mm poly-D-lysine–coated Petri dishes using DMEM (Life Technologies) with 10% heat-inactivated horse serum (Life Technologies), 5% fetal bovine serum (Atlanta Biologicals), and 1% penicillin/streptomycin. After 24 h of recovery, cells were differentiated using media containing DMEM, 1% heat-inactivated horse serum, and 1% penicillin/streptomycin. Added to this was a 1:1000 ratio of 100 ng/µl nerve growth factor (NGF) (Novoprotein). This was added to the cells a minimum of 24 h before measurements were taken.

Cells were viewed 2 d after plating and 1 d after treatment with nerve growth factor (NGF). Cells with minimal cell–cell contact were selected to reduce the mechanical impacts of cell communication. Three force curves in separate perinuclear regions with cantilever velocity of 2 µm/s and trigger point lnN were taken for each selected cell. Measurements were taken within 30 min of removal from the incubator to facilitate cell viability.

The stiffness of the measured cells E was determined from the force curve data utilizing the Hertz model for conical cantilever tip geometry,

$$E = kd\pi\left(1-\nu^2\right)/2\Delta^2 \tan\phi$$

where k is the cantilever spring constant, d is the cantilever deflection, ν is the Poisson's ratio (0.5 used for an assumed incompressible material), Δ is the sample indentation depth, and ϕ is the half-angle of the conical cantilever tip (35°). The force curves were processed using a custom MATLAB code that fits the indentation curve over a 500 nm range after manual selection of the initial contact point.

Fluorescence imaging of *Caenorhabditis elegans*

Worms were transferred into a microcentrifuge tube containing l mM carbachol and were submerged in the tube for 30 min at room temperature or in 100 mM NaCl solution for 10 min. After 30 or 10 min, respectively, the worms were removed from solution and placed on a glass slide with a thin layer of agar for the worms to lie on. Excess carbachol was wicked up from the pad and the worms were paralyzed using 25 M levamisole, which does not affect our pathway of interest. The worms were then imaged on an inverted confocal microscope and were visually checked for neurite rupture and retraction.

Chemotaxis assay of *Caenorhabditis elegans*

Worms were transferred to a new seeded plate 24 h before the experiment. The day of the experiment an unseeded plate was marked with a dot in the center and two circles on either ends of the plate with the "C" for control of DI water and "D" for diacetyl, which is the attractant. Using approximately 1 ml of S Basal (5.85 g NaCl, 1 g K_2HPO_4, 6 g KH_2PO_4, 1 ml cholesterol [5 mg/ml in ethanol], H_2O to 1 liter; sterilize by autoclaving; see Stiernagle, 2006), the worms were washed into a microcentrifuge tube and allowed to pellet for 5–10 min. Once pelleted, the worms were washed with S Basal two more times and finally with water. Suspended worms (10 µl) were transferred to the experimental plate previously made and the excess water was removed by wicking. The plate was then incubated for 45 min at 20°C, and afterward, the worms that moved to either the attractant or control were counted.

ACKNOWLEDGMENTS

This work was supported by National Institutes of Health grant GM116187 (S.S.) and Air Force Office of Scientific Research (AFOSR) MURI FA9550-18-1-0051 (P.R.) and R01DC016058 (J.S.). We thank various members of the Rangamani and Scarlata labs for valuable discussion and manuscript review. We thank Sayed Iman Mousavi (Yale University) and Erkan Tuzel (Temple University) for writing the Re-Track program. We thank the UCSD Interfaces Graduate Training Program and the San Diego Fellowship for funding and support for M.B. M.B. was also supported by a National Defense Science and Engineering Graduate (NDSEG) Fellowship, AFOSR Multidisciplinary Research Program of the University Research Initiative (MURI) grant FA9550-18-1-0051 to P.R., and the National Institutes of Health (Grant T32EB009380).

REFERENCES

Berstein G, Blank JL, Jhon D-Y, Exton JH, Rhee SG, Ross EM (1992). Phospholipase C-β1 is a GTPase-activating protein for $G_{q/11}$, its physiologic regulator. Cell 70, 411–418.

Bittner MA, Holz RW (2005). Phosphatidylinositol-4,5-bisphosphate: actin dynamics and the regulation of ATP-dependent and -independent secretion. Mol Pharmacol 67, 1089–1098.

Bornschlogl T, Romero S, Vestergaard CL, Joanny JF, Van Nhieu GT, Bassereau P (2013). Filopodial retraction force is generated by cortical actin dynamics and controlled by reversible tethering at the tip. Proc Natl Acad Sci USA 110, 18928–18933.

Brini M, Cali T, Ottolini D, Carafoli E (2014). Neuronal calcium signaling: function and dysfunction. Cell Mol Life Sci 71, 2787–2814.

Calabrese B, Saffin JM, Halpain S (2014). Activity-dependent dendritic spine shrinkage and growth involve downregulation of cofilin via distinct mechanisms. PLoS One 9, e94787.

Clapham DE (2007). Calcium signaling. Cell 131, 1047–1058.

Datar A, Ameeramja J, Bhat A, Srivastava R, Bernal R, Prost J, Callan-Jones A, Pullarkat PA (2019). The roles of microtubules and membrane tension in axonal beading, retraction, and atrophy. Biophys J 117, 880–891.

Diz-Munoz A, Fletcher DA, Weiner OD (2013). Use the force: membrane tension as an organizer of cell shape and motility. Trends Cell Biol 23, 47–53.

Dohlman HG, Thorner J (1997). RGS proteins and signaling by heterotrimeric G proteins. J Biol Chem 272, 3871–3874.

Drubin DG, Feinstein SC, Shooter EM, Kirschner MW (1985). Nerve growth factor-induced neurite outgrowth in PC12 cells involves the coordinate induction of microtubule assembly and assembly-promoting factors. J Cell Biol 101, 1799–1807.

Franze K, Gerdelmann J, Weick M, Betz T, Pawlizak S, Lakadamyali M, Bayer J, Rillich K, Gogler M, Lu YB, *et al.* (2009). Neurite branch retraction is caused by a threshold-dependent mechanical impact. Biophys J 97, 1883–1890.

Freedman NJ, Lefkowitz RJ (1996). Desensitization of G protein-coupled receptors. Recent Prog Horm Res 51, 319–351; discussion 352–313.

Garcia P, Gupta R, Shah S, Morris AJ, Rudge SA, Scarlata S, Petrova V, McLaughlin S, Rebecchi MJ (1995). The pleckstrin homology domain of phospholipase C-delta 1 binds with high affinity to phosphatidylinositol 4,5-bisphosphate in bilayer membranes. Biochemistry 34, 16228–16234.

Getz M, Swanson L, Sahoo D, Ghosh P, Rangamani P (2019). A predictive computational model reveals that GIV/girdin serves as a tunable valve for EGFR-stimulated cyclic AMP signals. Mol Biol Cell 30, 1621–1633.
Gilbert J, Man H-Y (2017). Fundamental elements in autism: from neurogenesis and neurite growth to synaptic plasticity. Front Cell Neurosci 11, 359–359.
Goldberg DJ, Grabham PW (1999). Braking news: calcium in the growth cone. Neuron 22, 423–425.
Gomez TM, Spitzer NC (1999). In vivo regulation of axon extension and pathfinding by growth-cone calcium transients. Nature 397, 350–355.
Greene LA, Tischler AS (1976). Establishment of a noradrenergic clonal line of rat adrenal pheochromocytoma cells which respond to nerve growth factor. Proc Natl Acad Sci USA 73, 2424–2428.
Grintsevich EE, Reisler E (2014). Drebrin inhibits cofilin-induced severing of F-actin. Cytoskeleton (Hoboken) 71, 472–483.
Guo Y, Rebecchi M, Scarlata S (2005). Phospholipase Cbeta2 binds to and inhibits phospholipase Cdelta1. J Biol Chem 280, 1438–1447.
Hartzell CA, Jankowska KI, Burkhardt JK, Lewis RS (2016). Calcium influx through CRAC channels controls actin organization and dynamics at the immune synapse. Elife 5, e14850.
Hassinger JE, Oster G, Drubin DG, Rangamani P (2017). Design principles for robust vesiculation in clathrin-mediated endocytosis. Proc Natl Acad Sci USA 114, E1118–E1127.
He L, Tao J, Maity D, Si F, Wu Y, Wu T, Prasath V, Wirtz D, Sun SX (2018). Role of membrane-tension gated Ca(2+) flux in cell mechanosensation. J Cell Sci 131, jcs208470.
Kadamur G, Ross EM (2013). Mammalian phospholipase C. Annu Rev Physiol 75, 127–154.
Kerstein PC, Nichol RI, Gomez TM (2015). Mechanochemical regulation of growth cone motility. Front Cell Neurosci 9, 244.
King AE, Woodhouse A, Kirkcaldie MT, Vickers JC (2016). Excitotoxicity in ALS: overstimulation, or overreaction? Exp Neurol 275(Pt 1), 162–171.
LaFerla FM (2002). Calcium dyshomeostasis and intracellular signalling in Alzheimer's disease. Nat Rev Neurosci 3, 862–872.
Licht T, Goshen I, Avital A, Kreisel T, Zubedat S, Eavri R, Segal M, Yirmiya R, Keshet E (2011). Reversible modulations of neuronal plasticity by VEGF. Proc Natl Acad Sci USA 108, 5081–5086.
Logan MR, Mandato CA (2006). Regulation of the actin cytoskeleton by PIP2 in cytokinesis. Biol Cell 98, 377–388.
Lohmann C, Wong RO (2005). Regulation of dendritic growth and plasticity by local and global calcium dynamics. Cell Calcium 37, 403–409.
Mattson MP (2007). Calcium and neurodegeneration. Aging Cell 6, 337–350.
McCullough BR, Blanchoin L, Martiel JL, De la Cruz EM (2008). Cofilin increases the bending flexibility of actin filaments: implications for severing and cell mechanics. J Mol Biol 381, 550–558.
McKay SE, Purcell AL, Carew TJ (1999). Regulation of synaptic function by neurotrophic factors in vertebrates and invertebrates: implications for development and learning. Learn Mem 6, 193–215.
Mikati MA, Grintsevich EE, Reisler E (2013). Drebrin-induced stabilization of actin filaments. J Biol Chem 288, 19926–19938.
Mutalik SP, Joseph J, Pullarkat PA, Ghose A (2018). Cytoskeletal mechanisms of axonal contractility. Biophys J 115, 713–724.
Nair RR, Patil S, Tiron A, Kanhema T, Panja D, Schiro L, Parobczak K, Wilczynski G, Bramham CR (2017). Dynamic arc SUMOylation and selective interaction with F-actin-binding protein drebrin A in LTP consolidation in vivo. Front Synaptic Neurosci 9, 8.
Nourse JL, Pathak MM (2017). How cells channel their stress: interplay between Piezo1 and the cytoskeleton. Semin Cell Dev Biol 71, 3–12.
Pavlov D, Muhlrad A, Cooper J, Wear M, Reisler E (2007). Actin filament severing by cofilin. J Mol Biol 365, 1350–1358.
Randlett O, Poggi L, Zolessi FR, Harris WA (2011). The oriented emergence of axons from retinal ganglion cells is directed by laminin contact in vivo. Neuron 70, 266–280.
Rangamani P, Fardin MA, Xiong Y, Lipshtat A, Rossier O, Sheetz MP, Iyengar R (2011). Signaling network triggers and membrane physical properties control the actin cytoskeleton-driven isotropic phase of cell spreading. Biophys J 100, 845–857.
Raucher D, Stauffer T, Chen W, Shen K, Guo S, York JD, Sheetz MP, Meyer T (2000). Phosphatidylinositol 4,5-bisphosphate functions as a second messenger that regulates cytoskeleton-plasma membrane adhesion. Cell 100, 221–228.
Rosenberg SS, Spitzer NC (2011). Calcium signaling in neuronal development. Cold Spring Harb Perspect Biol 3, a004259.
Sanchez-Fernandez G, Cabezudo S, Garcia-Hoz C, Beninca C, Aragay AM, Mayor F Jr, Ribas C (2014). Galphaq signalling: the new and the old. Cell Signal 26, 833–848.
Scarlata S (2019). The role of phospholipase Cβ on the plasma membrane and in the cytosol: How modular domains enable novel functions. Adv Biol Regul 73, 100636.
Scarlata S, Singla A, Garwain O (2018). Phospholipase Cβ interacts with cytosolic partners to regulate cell proliferation. Adv Biol Regul 67, 7–12.
Sengupta P, Samuel ADT (2009). *Caenorhabditis elegans*: a model system for systems neuroscience. Curr Opin Neurobiol 19, 637–643.
Sharma S, Grintsevich EE, Phillips ML, Reisler E, Gimzewski JK (2011). Atomic force microscopy reveals drebrin induced remodeling of f-actin with subnanometer resolution. Nano Lett 11, 825–827.
Sheetz MP (2001). Cell control by membrane–cytoskeleton adhesion. Nat Rev Mol Cell Biol 2, 392–396.
Sheetz MP, Dai J (1996). Modulation of membrane dynamics and cell motility by membrane tension. Trends Cell Biol 6, 85–89.
Simunovic M, Manneville JB, Renard HF, Evergren E, Raghunathan K, Bhatia D, Kenworthy AK, Voth GA, Prost J, McMahon HT, *et al*. (2017). Friction mediates scission of tubular membranes scaffolded by BAR proteins. Cell 170, 172–184.e111.
Stiernagle T (2006, February 11). Maintenance of *C. elegans*. In: WormBook: The Online Review of *C. elegans* Biology [Internet], Pasadena, CA, 2005–2018.
Stuchlik A (2014). Dynamic learning and memory, synaptic plasticity and neurogenesis: an update. Front Behav Neurosci 8, 106–106.
Takeuchi T, Duszkiewicz AJ, Morris RGM (2014). The synaptic plasticity and memory hypothesis: encoding, storage and persistence. Philos Trans R Soc Lond B Biol Sci 369, 20130288.
van Rheenen J, Jalink K (2002). Agonist-induced PIP(2) hydrolysis inhibits cortical actin dynamics: regulation at a global but not at a micrometer scale. Mol Biol Cell 13, 3257–3267.
Voglis G, Tavernarakis N (2006). The role of synaptic ion channels in synaptic plasticity. EMBO Rep 7, 1104–1110.
West AE, Chen WG, Dalva MB, Dolmetsch RE, Kornhauser JM, Shaywitz AJ, Takasu MA, Tao X, Greenberg ME (2001). Calcium regulation of neuronal gene expression. Proc Natl Acad Sci USA 98, 11024–11031.
Zmurchok C, Bhaskar D, Edelstein-Keshet L (2018). Coupling mechanical tension and GTPase signaling to generate cell and tissue dynamics. Phys Biol 15, 046004.